

Toward Efficient Enzymes for the Generation of Universal Blood through Structure-Guided Directed Evolution

David H. Kwan,^{†,‡} Iren Constantinescu,^{§,||} Rafi Chapanian,^{§,||} Melanie A. Higgins,[⊥] Miriam P Kötler,^{†,‡} Eric Samain,[#] Alisdair B. Boraston,[⊥] Jayachandran N. Kizhakkedathu,^{‡,§,||} and Stephen G. Withers^{*,†,‡}

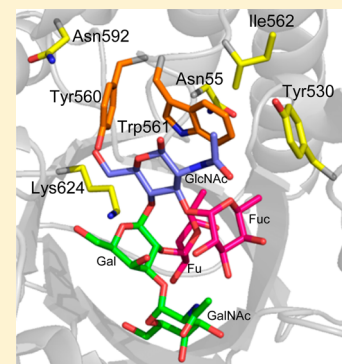
[†]Centre for High-Throughput Biology, [‡]Department of Chemistry, [§]Centre for Blood Research, ^{||}Department of Pathology and Laboratory Medicine, University of British Columbia, Vancouver, British Columbia, Canada V6T 1Z3

[⊥]Department of Biochemistry and Microbiology, University of Victoria, Victoria, British Columbia, Canada V8W 3P6

[#]Centre de Recherches sur les Macromolécules Végétales, Centre National de la Recherche Scientifique, Grenoble Cedex 9, France BP 53, 38041

S Supporting Information

ABSTRACT: Blood transfusions are critically important in many medical procedures, but the presence of antigens on red blood cells (RBCs, erythrocytes) means that careful blood-typing must be carried out prior to transfusion to avoid adverse and sometimes fatal reactions following transfusion. Enzymatic removal of the terminal *N*-acetylgalactosamine or galactose of A- or B-antigens, respectively, yields universal O-type blood, but is inefficient. Starting with the family 98 glycoside hydrolase from *Streptococcus pneumoniae* SP3-BS71 (Sp3GH98), which cleaves the entire terminal trisaccharide antigenic determinants of both A- and B-antigens from some of the linkages on RBC surface glycans, through several rounds of evolution, we developed variants with vastly improved activity toward some of the linkages that are resistant to cleavage by the wild-type enzyme. The resulting enzyme effects more complete removal of blood group antigens from cell surfaces, demonstrating the potential for engineering enzymes to generate antigen-null blood from donors of various types.



■ INTRODUCTION

The most clinically important antigens that must be considered when carrying out blood transfusions and tissue or organ transplantations are the A and B carbohydrate antigens of the ABO blood group system.¹ The antigenic determinant of each of these consists of a trisaccharide moiety attached to glycoproteins and lipids on the surface of red blood cells (RBCs) (Figure 1A). The trisaccharide of the A-antigen (GalNAc α -1,3-(Fuc α -1,2)-Gal β -) terminates with an *N*-acetylgalactosamine, whereas, in the B-antigen (Gal α -1,3-(Fuc α -1,2)-Gal β -), the terminal sugar is galactose. Glycans of O-type cells lacking this terminal sugar thus present the core Fuc α -1,2-Gal β - structure and are nonantigenic for the vast majority of individuals. These same ABO blood group antigens are also found on the glycans of endothelial and most epithelial cells.² The genotypes corresponding to the ABO blood group phenotypes can be defined by the A, B, and O alleles of a glycosyltransferase gene responsible for the addition of the terminal sugar in these structures. A and B alleles encode glycosyltransferases differing by a few amino acid substitutions, resulting in specific transfer of either GalNAc or Gal, respectively, whereas the O allele encodes a catalytically inactive protein.³ Individuals who lack A- or B-antigens produce antibodies to that missing antigen; thus, blood transfusions or tissue transplantation from an incompatible donor will result in an immune response, which can be fatal.

Enzymatic removal of the terminal *N*-acetylgalactosamine or galactose of A- or B- antigens, respectively, to generate O-type blood has long been proposed as a means of converting erythrocytes into a universal, antigen-null, donor type.⁴ Initial studies focused on the coffee bean α -galactosidase, as the only practically available enzyme at that time. While the principle was demonstrated for B-type blood, enormous quantities of enzyme were required to effect conversions.^{4a} Considerably more efficient enzymes for conversion of A and of B type blood that function at neutral pH were discovered by screening of bacterial libraries using specific oligosaccharide substrates.^{4b} However, even with these improved versions, up to 60 mg of enzyme was required per unit of RBC for the conversion of more recalcitrant A types.

Potential for a new enzymatic approach using a single enzyme for conversion of both A and B blood came with the discovery that *Clostridium perfringens*, a human gut pathogen, secretes an endo- β -galactosidase that removes the whole trisaccharide of the A- and B-antigens from host cell-surface glycans, leaving antigen-null red blood cells.⁵ This enzyme, the first discovered member of glycoside hydrolase family GH98, was dubbed an EABase, denoting its endoglycosidase activity on both A- and B-antigens. Homologues of this enzyme, exhibiting the same activity, have since been identified as

Received: November 11, 2014

Published: April 14, 2015

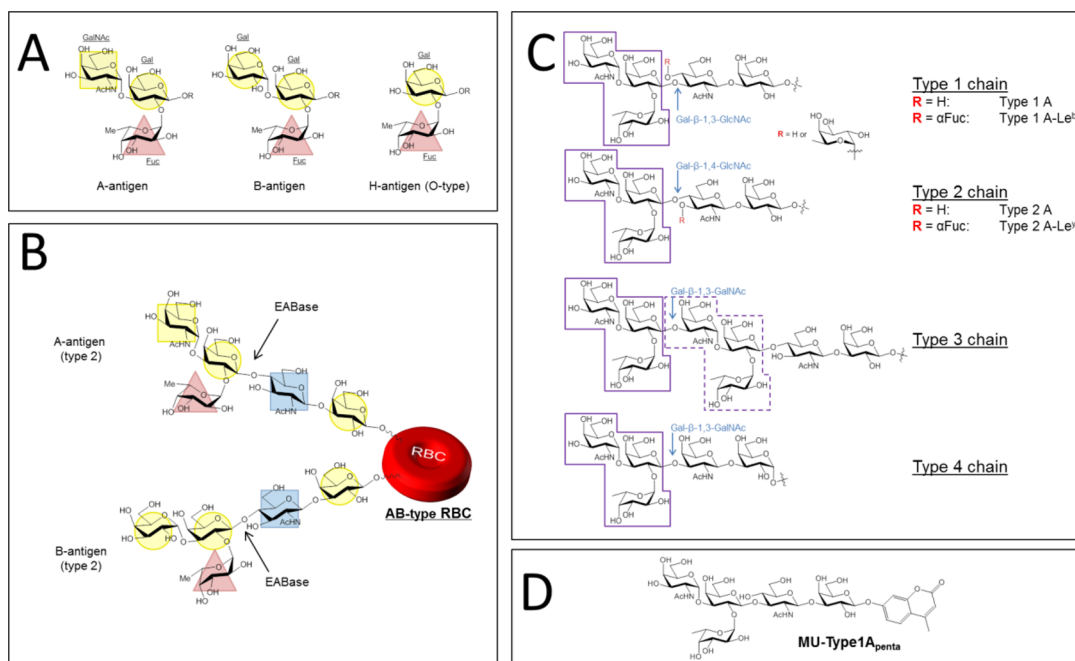


Figure 1. (A) Carbohydrate antigenic determinants of A-, B-, and H-antigens. The H-antigen is present on glycans of the O blood-group, and typically nonantigenic except in rare cases. (B) Site of cleavage of A- and B-antigens by GH98 EABase enzymes from type 2 chains of erythrocytes. (C) Various chain types to which A-antigens are present on erythrocytes and other cell types. (D) Structure of the fluorogenic substrate MU-Type1A_{penta}.

virulence factors in some strains of *Streptococcus pneumoniae*.⁶ These enzymes are efficient catalysts for cleaving the Gal β -1,4-GlcNAc linkage by which the A- and B-antigen trisaccharide is attached to the (type 2) inner core oligosaccharide of cell-surface glycans (Figure 1B).^{2,7} However, the presence of other linkages by which the trisaccharide is linked to the glycan, as described below, can affect the activity of EABase and of other enzymes (Figure 1C).

Although the majority of A- and B-trisaccharide antigens are linked to RBC glycans by a Gal β -1,4-GlcNAc linkage (type 2 chain), they can also be linked by a Gal β -1,3-GlcNAc linkage (type 1 chain) and by a Gal β -1,3-GalNAc linkage (type 3 and type 4 chains). The presence or absence of blood group antigens on type 1, 3, and 4 chains varies from person to person, while the distribution of chain types varies with tissue or cell type.² Erythrocytes do not synthesize the type 1 A- or B-antigens, but rather absorb them from glycolipids circulating in the plasma of individuals with a secretor phenotype (they produce soluble ABO antigens in plasma as well as in secretions such as saliva).^{7a,8} The A-antigen is also present on type 3 and 4 chains in individuals of subgroup A₁, a phenotype which distinguishes them from subgroup A₂ individuals in whom these chains are absent.^{2,7b,9}

The type 1, 3, and 4 chain linkages, in which the trisaccharide antigenic determinant is linked to the core oligosaccharide by a Gal β -1,3 linkage (Gal β -1,3-GlcNAc in type 1 and Gal β -1,3-GalNAc in types 3 and 4), are only very slowly hydrolyzed by EABase compared to the Gal β -1,4 linkage of the type 2 chain. In order to improve the utility of EABase as a tool for generating universal donor blood and tissues, we have sought to enhance the activity toward Gal β -1,3 linkages. In the present work, we report the directed evolution of the EABase Sp3GH98, from *Streptococcus pneumoniae* SP3-BS71. We demonstrate that through several iterations of structure-guided, site-selected randomized mutagenesis, in conjunction with a

high-throughput screen, we are able to isolate mutant enzymes with improved activity toward the A-antigen on type 1 chains. The most improved mutant exhibits 170-fold higher activity toward the cleavage of the Gal β -1,3-GlcNAc linkage in a small-molecule oligosaccharide substrate consisting of the five terminal glycoside residues of the type 1 A blood group antigen linked at the reducing end to a methylumbelliferyl fluorogenic reporter (while retaining activity toward a type 2 A blood group antigen substrate to within an order of magnitude of the wild-type enzyme). We also show here that these improved enzymes have superior catalytic properties in the cleavage of antigens from type 1 A-antigen-expressing cells, where immunofluorescence assays demonstrate the improved, though still incomplete, removal of A-antigens bearing this linkage. This work thus presents a promising proof-of-concept for developing more efficient catalysts for blood group antigen removal.

RESULTS

Microtiter Plate-Based High-Throughput Screening Assay for the Directed Evolution of Sp3GH98. In order to engineer the EABase, Sp3GH98, from *S. pneumoniae* SP3-BS71 for improved activity toward cleavage of the Gal β -1,3-GlcNAc linkage of type 1 A-antigens by directed evolution, a high-throughput assay was required. The assay we developed utilized a fluorogenic substrate (MU-Type1A_{penta}) consisting of the type 1 A blood group pentasaccharide linked by a β -glycosidic bond to a methylumbelliferyl moiety (Figure 1D). Cleavage of this substrate by an EABase would release the A trisaccharide from the substrate, allowing the coexpressed coupling enzymes β -hexosaminidase and β -galactosidase to sequentially cleave the disaccharide product yielding *N*-acetylglucosamine and galactose, along with fluorescent methylumbelliferone. This process could be monitored fluorimetrically. The required methylumbelliferyl pentasaccharide, MU-Type1A_{penta}, was

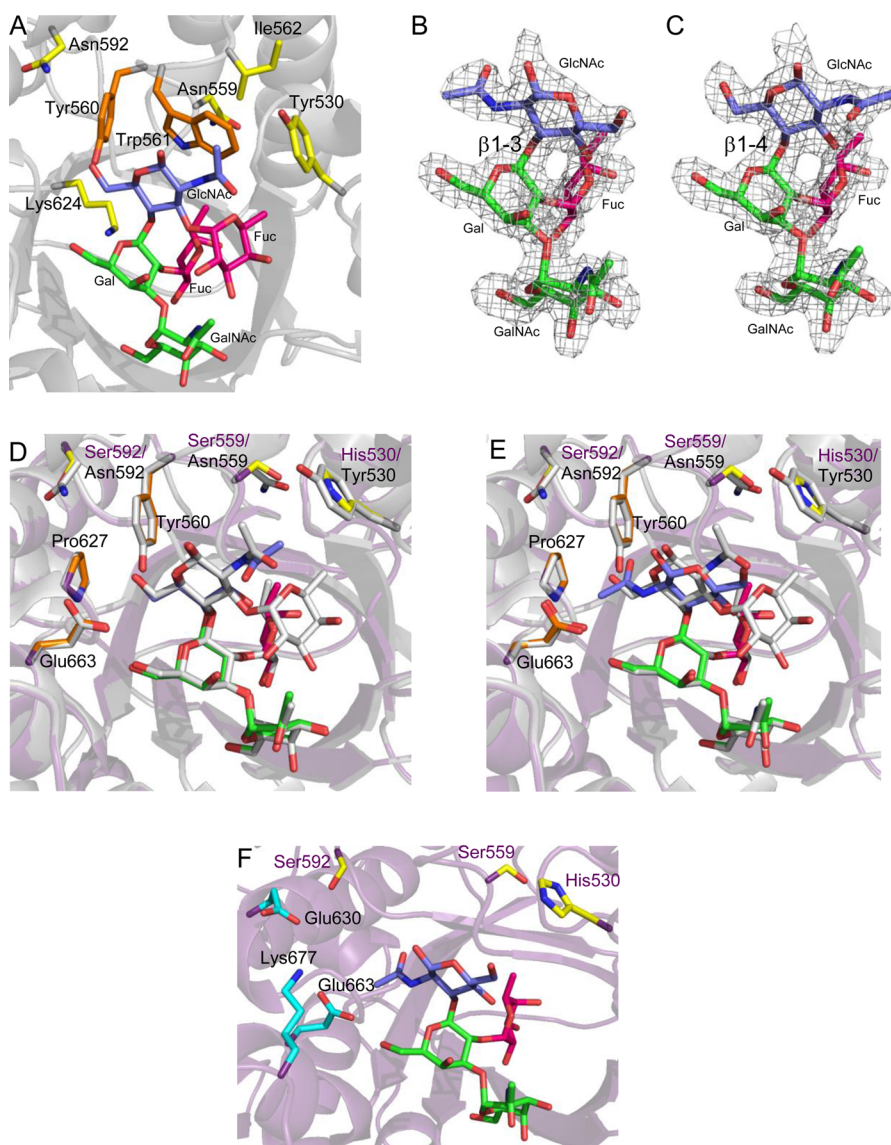


Figure 2. Structural analysis of Sp3GH98 and mutants. (A) Structure of Sp3GH98E558A in complex with type 2 blood group A-Lewis^Y antigen (PDB ID 2WMK). The amino acid residues chosen for randomization are shown as sticks with those in the first shell colored orange and those in the second shell colored yellow. (B and C) $F_o - F_c$ electron density maps contoured at 3.5σ for the type 1 blood group A tetrasaccharide (B) and type 2 blood group A tetrasaccharide (C) in complex with the 2.5-L19 mutant bearing an additional E558A mutation to inactivate the enzyme. (D) Structural overlay of the 2.5-L19E558A mutant in complex with the type 2 blood group A tetrasaccharide with Sp3GH98E558A in complex with the A-Lewis^Y antigen. The Sp3GH98E558A backbone (cartoon representation), relevant side chains, and carbohydrate are shown in gray. The 2.5-L19 backbone (cartoon representation) is shown in purple, and the mutated residues in 2.5-L19 are shown as yellow sticks (purple labels). Residues in the pocket accommodating the O6 or acetamido groups are shown as orange sticks. (E) Same as panel D but 2.5-L19E558A is in complex with the type 1 blood group A tetrasaccharide. (F) Structure of 2.5-L19E558A in complex with the type 1 blood group A tetrasaccharide with mutated residues shown as yellow sticks. Residues chosen for subsequent rounds of randomization are shown as blue sticks. In all panels, the carbohydrate is shown as sticks with Gal and GalNAc residues colored green, GlcNAc colored blue, and Fuc colored red.

obtained using an engineered *E. coli* cell line expressing the requisite glycosyltransferases as described in the Supporting Information (Figure S1). The coupling enzymes were included by coexpression of the mutant variants of Sp3GH98 with a plasmid-encoded β -hexosaminidase from *Streptococcus pneumoniae* and the endogenous β -galactosidase in *E. coli*. This allowed us to directly assay the activity of the mutants by addition of the pentasaccharide substrate to lysed cell extracts, followed by measurement of the fluorescence released over time.

Design and Screening of Libraries Based upon the Crystal Structure of the Parent Enzyme in Complex with the Type 2 A Oligosaccharide. The availability of the crystal

structure of Sp3GH98 solved in complex with the type 2 A-Lewis^Y pentasaccharide (PDB ID 2WMK) allowed a structure-guided approach to be used to target residues for iterative site-saturation mutagenesis (as described by Reetz and Carbal-leira¹⁰) (Figure 2A).⁶ This structure revealed the residues that provide primary contacts (first shell) with the sugars in the +1 and +2 subsites, as well as those residues in the second shell that orient the primary residues for substrate recognition. Because of the difference in the linkage of the type 1 A versus the type 2 A blood group oligosaccharide, the orientations of the sugars that bind in the +1 and +2 subsites must differ between type 1 and 2 chains. We therefore sought to remodel

Table 1. Identity of Mutants and Their Activity against MU-Type1A_{penta}

Variant	Amino acid residue identity at targeted positions						k_{cat} (s ⁻¹) ($\times 10^{-3}$)	K_m (mM)	k_{cat}/K_m (s ⁻¹ mM ⁻¹)	Fold over WT
	530	559	592	630	677	692				
Wild-type	Tyr	Asn	Asn	Glu	Lys	Leu	1.3 ± 0.1	3.7 ± 0.3	3.7 × 10 ⁻⁴	1
1.1-L07	Tyr	Ser	Asn	Glu	Lys	Leu	1.3 ± 0.1	1.3 ± 0.1	1.0 × 10 ⁻³	2.7
1.1-I02	Tyr	Asn	Val	Glu	Lys	Leu	1.4 ± 0.02	1.4 ± 0.1	1.0 × 10 ⁻³	2.7
1.2-O22	Tyr	Asn	Ser	Glu	Lys	Leu	1.6 ± 0.1	1.5 ± 0.2	1.1 × 10 ⁻³	3.0
2.0-X01	Tyr	Ser	Val	Glu	Lys	Leu	2.0 ± 0.1	0.9 ± 0.1	2.2 × 10 ⁻³	5.9
2.0-X02	Tyr	Ser	Ser	Glu	Lys	Leu	1.8 ± 0.1	0.7 ± 0.1	2.4 × 10 ⁻³	6.5
2.5-L19	Ile	Ser	Ser	Glu	Lys	Leu	2.3 ± 0.1	0.8 ± 0.1	2.8 × 10 ⁻³	7.6
3.1-I24	Ile	Ser	Val	Gln	Lys	Leu	1.5 ± 0.1	0.31 ± 0.03	4.9 × 10 ⁻³	13
3.1-M04	Ile	Ser	Val	Leu	Lys	Leu	1.5 ± 0.1	0.26 ± 0.03	5.7 × 10 ⁻³	15
3.8-B22	Ile	Ser	Phe	Trp	Lys	Leu	2.2 ± 0.1	0.32 ± 0.05	6.9 × 10 ⁻³	19
4C.1-O14	Ile	Ser	Val	Gln	Leu	Leu	18 ± 1	0.9 ± 0.1	1.9 × 10 ⁻²	51
4A.1-B17	Ile	Ser	Val	Leu	Arg	Leu	4.0 ± 0.1	0.20 ± 0.02	2.0 × 10 ⁻²	54
4A.1-F01	Ile	Ser	Val	Leu	Arg	Leu	16 ± 0.4	0.5 ± 0.3	2.9 × 10 ⁻²	78
4B.1-E17	Ile	Ser	Phe	Trp	Arg	Leu	15 ± 1	0.46 ± 0.05	3.1 × 10 ⁻²	84
4A.1-D15	Ile	Ser	Val	Leu	Leu	Leu	17 ± 0.4	0.38 ± 0.02	4.6 × 10 ⁻²	120
5E.3-N06	Ile	Ser	Val	Leu	Leu	Ile	19 ± 1	0.30 ± 0.02	6.3 × 10 ⁻²	170

the +1 and +2 subsites to optimize binding and enzymatic turnover of the type 1 A oligosaccharide by mutating the residues within those sugar-binding subsites. Seven residues were chosen for randomization: in the first shell, residues Tyr560 and Trp561; and in the second shell Tyr530, Asn559, Ile562, Asn592, and Lys624 (Figure 2A). Using the wild-type Sp3GH98 gene as a template, site-saturation mutagenesis was performed at each of these positions individually. The resulting mutants were then pooled into a library in which each member potentially encoded a mutation in one of these seven residues. The mutants of this library were then expressed in *E. coli* and screened on 384-well plates. Three single-residue mutants, N559S, N592 V, and N592S (designated 1.1-L07, 1.1-I02, and 1.2-O22, respectively), with approximately 3-fold improved hydrolytic activity toward MU-Type1A_{penta} (as measured by k_{cat}/K_m) were identified from our screening of this library. Improvements were primarily due to a decrease in the K_m (Table 1 and Figure 3). Combination of the N559S mutation with either the N592 V or N592S mutations yielded double mutants (2.0-X01 and 2.0-X02, respectively) with roughly 6-fold improved activity over the wild-type, mostly due to further decreases in K_m (Table 1 and Figure 3). These double mutants were used as the template for a further round of site-saturation mutagenesis. Mutations in positions 559 and 592 were retained while site-saturation mutagenesis was performed for residues Tyr530, Tyr560, Trp561, Ile562, and Lys624 individually and pooled into the second site-saturation library. Screening revealed a triple mutant, 2.5-L19, which encoded Y530H, N559S, and N592S replacements and had moderately further improved activity, totaling nearly 8-fold that of wild-type. With

these improvements, structural analysis of complexes of type 1 A oligosaccharides was thought to now be possible, which could help in mutant library design for the next round of mutagenesis.

Crystal Structure of Mutant Enzymes in Complex with the Type 1 A Oligosaccharide. To obtain crystal structures in complex with the A oligosaccharide, catalytically inactive mutants were generated from 2.0-X01, 2.0-X02, and 2.5-L19 by mutation of the catalytic acid residue⁶ to an alanine E558A. The improved binding of 2.0-X01, 2.0-X02, and 2.5-L19 toward the type 1 A oligosaccharide compared to wild-type, as observed by a 4- to 5-fold decrease in K_m for MU-Type1A_{penta} (which is in the submillimolar range for those mutants), allowed us to capture the type 1 A tetrasaccharide–enzyme complex in crystallographic studies with the E558A variants (PDB IDs 4d6f, 4d6h, 4d6i) in addition to the type 2 A tetrasaccharide–enzyme complex (PDB IDs 4d6j, 4d71, 4d47) (Figure 2B and 2C and Supporting Information Figure S4). Interestingly very few differences in protein structure were seen between the evolved mutants and the parent apo enzyme or in complexes with type 1 A or type 2 A oligosaccharides (Figure 2D and 2E). However, the bound orientation of the type 1 A oligosaccharide was quite different from that of the type 2 (Figure 2B and 2C). Most notably, the *N*-acetylglucosamine in the +1 binding site is rotated 180° between the type 1 A and type 2 A oligosaccharides, such that the acetamide moiety of that sugar extends in the opposite direction. This would necessarily affect the positioning of the galactose residue in the +2 site, though our crystal structure does not include this sugar. In order to stabilize this bound conformation, we selected residues Glu630, Glu663, and Lys677 as candidates for mutation to provide

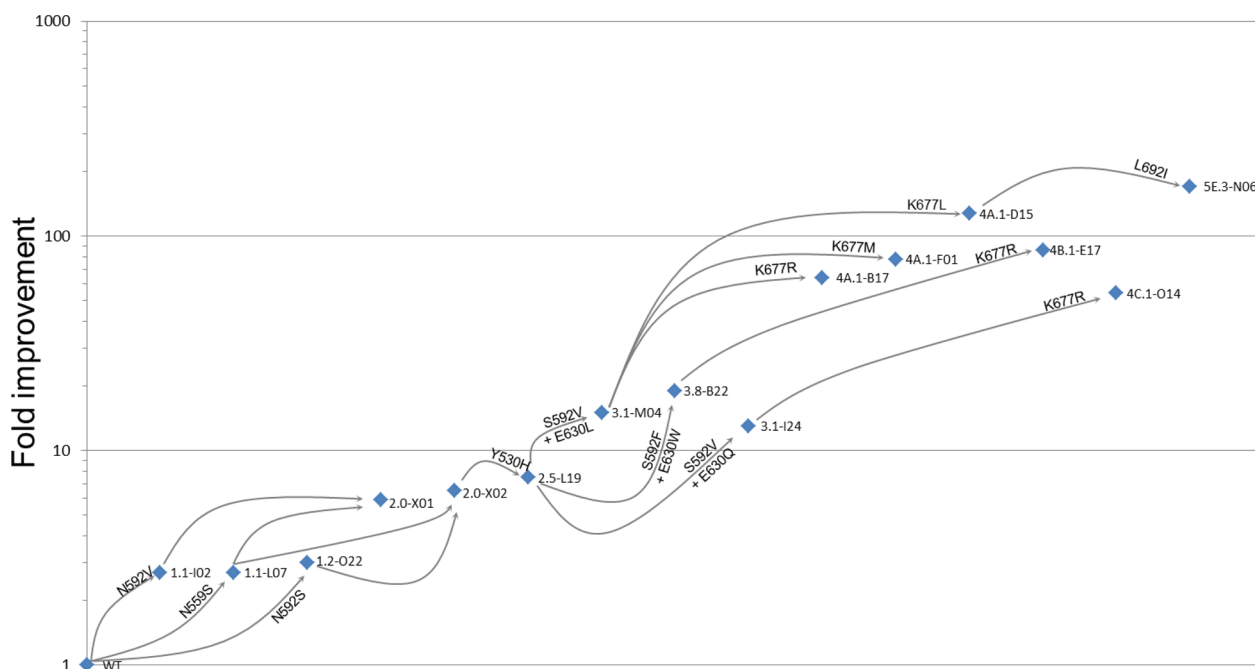


Figure 3. Evolutionary pathway of Sp3GH98 from five rounds of directed evolution. The first round of mutagenesis was screened from a library of mutants with mutations in one of the residues Tyr530, Asn559, Tyr560, Trp561, Ile562, Asn592, and Lys624. The improved mutants from the first round were recombined and then used as a template for a second round, in which a library was generated in which members had mutations in one of the residues Tyr530, Tyr560, Trp561, Ile562, and Lys624. The best mutant from the second round was further mutated simultaneously in residues 592 and 630 for the third round, and mutants from the third round were simultaneously mutated in residues 663 and 677 for the fourth round. Finally the best mutant from the fourth round was subjected to error-prone PCR for the fifth round, from which the best mutant, SE.3-N06 was isolated.

stabilizing interactions (either through primary, or solvent-mediated contacts) with the flipped *N*-acetylglucosamine in the +1 site and its reoriented acetamide moiety, as well as to a repositioned galactose in the +2 site (Figure 2F).

Design and Screening of Libraries Based upon the Crystal Structure of a Mutant Enzyme in Complex with the Type 1 A Oligosaccharide. In the next rounds of directed evolution, using mutant 2.5-L19 as a template, we chose to randomize pairs of amino acid positions in order to probe potential cooperative interactions between mutated residues. Pairs of spatially close amino acid residues were corandomized using the process of Combinatorial Active-site Saturation Test (CAST) described by Reetz et al.¹¹ CAST is a structure-based method of designing mutant libraries for directed evolution in which spatially close amino acids are mutated simultaneously such that additive or synergistic effects of multiple mutations can be screened. As the chosen Glu630 residue was spatially close to the previously randomized position 592 (from the first round of mutagenesis) (Figure 2F), we chose to mutate these positions together to generate a combinatorial library. Screening of this library afforded three mutants, 3.1-I24, 3.1-M04, and 3.8-B22, with 13- to 19-fold improved activity over wild-type (again mostly due to lowered K_m) in which Asn592 was mutated to either valine (3.1-I24 and 3.1-M04) or phenylalanine (3.8-B22) and Glu630 to glutamine (3.1-I24), leucine (3.1-M04), or tryptophan (3.8-B22) (Table 1 and Figure 3). These three mutants were then used as the parents for a subsequent round of mutagenesis and screening using the CAST method in which the spatially close Glu663 and Lys677 (Figure 2F) were mutated together, yielding five further mutants, 4A.1-B17, 4A.1-D15, 4A.1-F01, 4B.1-E17, and 4C.1-O14, with 51- to 124-fold improved activity over the wild-

type enzyme (Table 1 and Figure 3). In contrast to mutants obtained from previous iterations of directed evolution, these variants showed considerably higher k_{cat} values. None of these mutants carried an amino acid replacement for Glu663, suggesting perhaps that any mutation in this position either produces unfavorable interactions or loses important interactions (likely to the 6-OH of the galactose in the -1 site, based on the crystal structure). The parentage of these mutants and their amino acid substitutions is summarized in Figure 3 and Table 1.

The mutant 4A.1-D15, whose k_{cat}/K_m value is 124-fold higher than that of the wild-type, was used as the parent for a final round of mutagenesis, this time using error-prone PCR. Screening of an error prone library of mutants encoding on average three base-pair substitutions per gene, generated a modestly improved mutant, SE.3-N06, bearing an additional L692I mutation, resulting in a total 170-fold greater activity than the wild-type enzyme (as measured by k_{cat}/K_m with respect to substrate MU-Type1A_{penta}) (Table 1 and Figure 3). Given the high mutational load, we were concerned that its stability might be badly compromised. Melting temperature studies revealed a T_m of 44 °C, which is perfectly adequate for use under the conditions in which erythrocytes would be treated (Supporting Information Figure S5). Despite our efforts, we were unable to generate diffraction quality crystals of the SE.3-N06 mutant. This may be due in part to increased flexibility of the mutant compared to its parent enzyme, which would be in agreement with the melting temperature studies. We also wished to determine whether improvements toward the type 1 A oligosaccharide had come at the cost of significant activity loss toward the type 2 A oligosaccharide. Kinetic studies using a fluorogenic substrate, MU-type2A_{tetra} (Figure S1),

consisting of the type 2 A tetrasaccharide (bearing the Gal β -1,4-GlcNAc linkage preferred by the parent enzyme) linked to a methylumbelliferyl moiety, indicate that while the SE.3-N06 mutant has lower activity toward this substrate ($k_{\text{cat}} = (0.95 \pm 0.03) \text{ s}^{-1}$; $K_m = (10 \pm 1) \mu\text{M}$) compared to the wild-type ($k_{\text{cat}} = (13 \pm 2) \text{ s}^{-1}$; $K_m = (29 \pm 9) \mu\text{M}$), the activity as measured by k_{cat}/K_m remains within the same order of magnitude. The consequence is a balancing of the activities of the enzyme toward the two linkages, allowing more complete removal of antigens.

Immunofluorescence and Immunohistochemical Detection of Blood Group Antigen Removal from Cell Surfaces. In order to demonstrate that the mutant enzymes improve the removal of type 1 A antigens from the surface of cells, we employed immunofluorescence using antibodies that are each specific to one of the type 1, 2, and 3 chains with minimal cross-reactivity to the others (Table 2). AH21 and

Table 2. Chain Specific Antibodies Used for Immunofluorescence Assays

Antigen(s)	Antibody
Type 1 A	AH21
Type 1 A-Le ^b	HH3
Type 2 A, Type 2 A-Le ^y	HH4
Type 3 A	TH1

HH3 are antibodies (IgM and IgG, respectively) with specificities toward type 1 A and type 1 A-Le^b antigens, respectively, whereas HH4 is an IgG antibody with specificity toward both type 2 A and type 2 A-Le^y antigens, and TH1 is an IgG antibody with specificity toward type 3 chains. With the exception of TH1, the sensitivity of these specific antibodies is not sufficient to detect their corresponding antigens on erythrocytes. We therefore used a cell line, A431 (derived from a squamous carcinoma), which expresses type 1 and type 2 A antigens in high titers. A431 cells, immobilized on glass slides, were treated with variants of the Sp3GH98 enzyme (either parent wild-type or mutant enzymes) in the presence of dextran (40 kDa average molecular weight) as a macromolecular crowder (which has been shown to enhance enzyme activity on cell surfaces¹²). Following washing, antigens were detected by binding of antitype 1 A or antitype 2 A antibodies and subsequent binding of a fluorescent FITC-labeled secondary (anti-IgG or -IgM) antibody. As seen in Figure 4, these immunofluorescence experiments using AH21 and HH3 antibodies show visibly improved removal of type 1 A antigens from cell surfaces. Although removal of the type 1 A antigen from the cell surfaces remained incomplete, measurable improvement was observed for the evolved enzyme with the best mutant, SE.3-N06, removing a substantial majority of the type 1 A antigen and the type 1 A-Le^b antigen (Figure 4A and 4B). Experiments with the antitype 2 A antibody, HH4, show that the type 2 A antigen is efficiently removed by both wild-type and SE.3-N06 (Supporting Information Figure S6). In contrast, immunofluorescence experiments on erythrocytes using the antitype 3 A antibody, TH1, showed that the mutant enzymes do not remove type 3 A antigens from the cell surface, nor does the parent wild-type enzyme (data not shown). That we did not identify mutants with improved activity toward A-antigens on type 3 or 4 chains should not be surprising, as screening had been for activity against the type 1 A antigen. These results warrant further engineering efforts in developing

a mutant enzyme capable of removing the type 3 and 4 linkages.

To test whether the activity of the mutant SE.3-N06 toward B blood group antigens differed from that of the wild-type enzyme, agglutination studies were carried out using anti-B antibodies on B blood group erythrocytes that had been treated with either the wild-type Sp3GH98 or the SE.3-N06 mutant in the presence of dextran. These tests indicated that, like the wild-type enzyme, SE.3-N06 could fully remove the B antigen from red blood cells beyond the limits of detection (Figure S7), albeit at increased enzyme concentration (consistent with the lower activity observed in the mutant toward the type 2 chain linkage in general).

DISCUSSION

Enzymatic removal of ABO blood group antigens has long held the promise of obviating the need to properly match blood donors for transfusions.^{4a} However, difficulties arise in this strategy due to the inefficiency of available enzymes used to catalyze cleavage of the carbohydrate antigens.¹³ One approach to address this limitation that has been explored uses molecular crowding polymers to improve the general activity of enzymatic reactions on cell surfaces by enhancing the association and binding of the enzymes on cell surfaces.¹² However, this approach does not improve intrinsic enzyme specificities and activities. In this report, we have explored a complementary approach to enhance the intrinsic activity of a blood group antigen-cleaving enzyme for specific linkage types through enzyme engineering by means of directed evolution.

The GH98, EABase homologue of *Streptococcus pneumoniae* SP3-BS71, Sp3GH98, is a highly efficient enzyme that cleaves both the A- and B-trisaccharide antigen from the type 2 core chain on which the majority of blood group antigens are displayed on erythrocytes. Though the parent enzyme's specificity toward the Gal β -1,4-GlcNAc linkage of the type 2 chain appears to be strict, through directed evolution, we have been able to broaden the specificity of the enzyme to allow it to more efficiently cleave the Gal β -1,3-GlcNAc linkage of type 1 chains. The previously determined low, but detectable, activity of wild-type EABases toward type 1 chains^{10,12} allowed us to utilize a coupled assay to screen for improved endoglycosidase activity from mutant libraries. We observed up to a 170-fold improvement in the activity (k_{cat}/K_m) of the evolved mutants compared to the wild-type on a small-molecule oligosaccharide substrate bearing this linkage. Many of the identified mutants had improved activity as a result of a decrease in K_m . This is likely a consequence of the use of a low substrate concentration during screening, though improvements in k_{cat} were observed in the later generations. By immunofluorescence, we saw increased cleavage of type 1 A chains from cell surfaces, although removal from cell surfaces remained incomplete. The very low activity of the parent wild-type enzyme for the type 1 chains is a substantial hurdle for complete removal, but our evolved enzymes are much closer to this goal. This is a significant step toward developing Sp3GH98 for the complete removal of blood group antigens, allowing for blood transfusions, and organ and tissue transplants from donors that would otherwise be mismatched.

In contrast with enzymatic removal of the terminal N-acetylgalactosamine or galactose of A- or B-antigens by N-acetylgalactosaminidases or galactosidases, respectively, the endoglycosidase activity of GH98 EABase enzymes such as Sp3GH98 removes the entire terminal trisaccharide of either

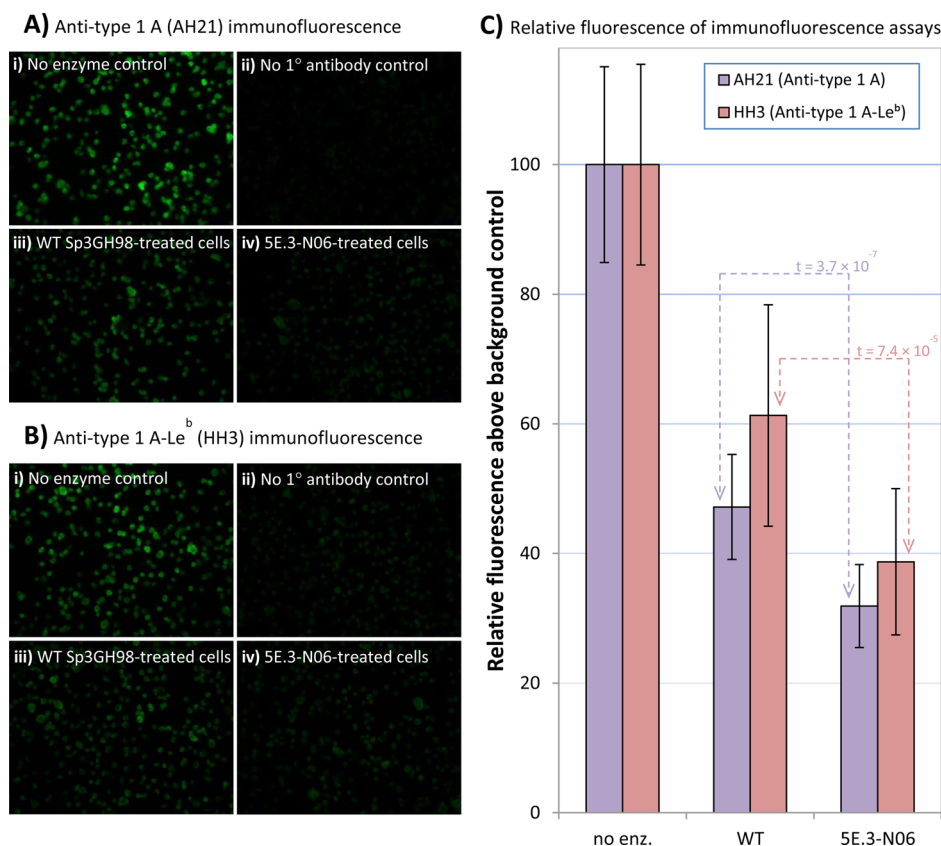


Figure 4. Immunofluorescence tests of A431 cells (derived from a squamous carcinoma) using the type 1 A-specific AH21 antibody (A) or the type 1 A-Le^b-specific HH3 antibody (B). In panel (i), cells were not treated with enzyme before immunofluorescence. In panel (ii), cells without enzyme treatment are shown where the primary antibody (either AH21 or HH3) was omitted prior to treatment with the secondary antibody (either FITC-labeled anti-IgG or FITC-labeled anti-IgM). In panel (iii), wild-type Sp3GH98-treated cells were subjected to immunofluorescence (treatment with either AH21 followed by FITC-labeled anti-IgM or HH3 followed by FITC-labeled anti-IgG). In panel (iv), 5E.3-N06-treated cells were subjected to immunofluorescence (treatment with either AH21 followed by FITC-labeled anti-IgM or HH3 followed by FITC-labeled anti-IgG). Relative fluorescence levels of immunofluorescence assays are shown (C), and the statistical significances of differences in measurements were verified by a Student's *t* test.

the A- or B-antigen. The glycans that result, strictly speaking, are not those of blood group O cells (H-antigen) but will nonetheless be unreactive to A or B antigens. It will be important, in future work, to confirm that cells converted by this treatment elicit no negative response following transfusion. If so, further remodeling of cell-surface carbohydrates may be warranted.

In addition to being present on the RBCs of individuals exhibiting a “secretor” phenotype (roughly 80% of the population), type 1 chains are widely distributed on endodermally derived tissue such as lining epithelia and glandular epithelia.² Thus, efficient removal of blood group antigens on type 1 chains by the engineered Sp3GH98 variants may also prove useful for tissue and organ transplantation. ABO-incompatible organ transplantation, whereby an individual receives an organ transplant from a donor of a conventionally incompatible blood type, is a procedure that allows a patient to receive a potentially life-saving transplant when organs from blood matched donors are unavailable. This procedure has been most successful for infant recipients, whose immune system has not yet fully developed.¹⁴ In adults, this procedure can be achieved with the prior removal of circulating antibodies by plasmapheresis, whereby blood is withdrawn and blood cells are separated from plasma and then returned to circulation with a plasma substitute.¹⁵ In cases where initial

graft rejection does not occur, it has been found that the grafted organ may persist without rejection even when antibodies against donor-specific blood group antigens return to pretransplant levels. This phenomenon, dubbed “accommodation”, has been postulated to be mediated by the expression of “protective genes” in the graft tissue, including genes that prevent inflammation, cell death, and immune activation.¹⁶ Thus, removal of blood group antigens from donor organs or tissues for transplantation may facilitate ABO-incompatible organ transplantation in avoiding initial rejection such that accommodation of the allografted organ can occur prior to the regeneration of antigens on the living donor tissue (which would not occur in red blood cells that lack a nucleus and most organelles¹⁷). We have demonstrated that, by directed evolution, we can broaden the substrate specificity of Sp3GH98 to cleave the Gal β -1,3-GlcNAc linkage of type 1 chains while retaining high activity toward the Gal β -1,4-GlcNAc linkage of the type 2 chains. This augurs well for future enzyme engineering efforts to further broaden the substrate specificity toward the Gal β -1,4-GalNAc linkage of type 3 and 4 chains on which A-antigens (but not B-antigens) are found in some individuals (belonging to the A₁ phenotype making up 80% of blood group A). Toward that aim, this work represents the first steps toward complete removal of all ABO blood group antigens with a single enzyme.

CONCLUDING REMARKS

Enzymatic removal of blood group antigens from erythrocytes is an attractive method for allowing for the transfusion of blood from an otherwise incompatible donor. However, glycosidase enzymes discovered from nature as yet have practical limitations toward this application. The results of our work in engineering the family 98 glycoside hydrolase from *Streptococcus pneumoniae* SP3-BS71 establish that directed evolution of enzymes acting upon blood group antigens can be an effective means of developing these catalysts toward practical application in generating universal blood.

METHODS

Synthesis of Methylumbelliferyl Oligosaccharides. The required methylumbelliferyl type 1 A blood group pentasaccharide, MU-Type1A_{penta} (Figure S1A) was obtained by feeding methylumbelliferyl β -galactoside to the *E. coli* cell line SD161¹⁸ expressing the five following genes: the β -1,3-*N*-acetylglucosaminyltransferase *lgtA* gene from *Neisseria meningitidis* MC58, the β -1,3-galactosyltransferase gene from *Helicobacter pylori* ATCC43504, the α -1,2-fucosyltransferase *futC* gene from *Helicobacter pylori* ATCC26695, the UDP-*N*-acetylglucosamine C4 epimerase from *Campylobacter jejuni* NCTC 11168, and the human α -1,3-*N*-acetylgalactosaminyltransferase *gtA* gene (Figure S1B). All these genes were expressed on three compatible plasmids under the control of the lactose promoter (Plac). The strain SD161 also had a chromosomally inserted Plac upstream of the four genes (*gmd*, *wcaG*, *manC*, and *manB*) involved in GDP-fucose biosynthesis to ensure GDP-fucose production upon Plac induction. The strain SD161 was grown at high cell density as previously described,^{18b} and methylumbelliferyl β -galactoside (2g/L) was added after induction of the blood group glycosylation system. After 24 h of culture with a constant glycerol feeding (3 g l⁻¹ h⁻¹), the cells were harvested by centrifugation. Methylumbelliferyl pentasaccharide was extracted from the cells which were permeabilized by a 20 min boiling treatment. The extract was acidified to pH 3.0 by addition of Amberlite IR120 (H⁺ form) resin to precipitate proteins which were removed by centrifugation. The clear supernatant was loaded on a C18 Reveleris Silica (120 g) column, and elution was carried out with a linear gradient from 100% water to 100% methanol with a flow rate of 80 mL/min for 35 min. Elution was monitored with an UV detector at 320 nm, and the presence of the methylumbelliferyl pentasaccharide in collected fractions was checked by TLC analysis. The final yield from this purification was 330 mg of MU-Type1A_{penta} (starting from one liter of culture).

The methylumbelliferyl type 2 A blood group tetrasaccharide MU-Type2A_{tetra} (Figure S1A) was synthesized chemoenzymatically from methylumbelliferyl β -*N*-acetyl-D-glucosaminopyranoside, α -D-galactosyl fluoride, GDP-fucose, and UDP-*N*-acetyl-D-galactosamine using the glycosynthase Abg-2F6,¹⁹ and the glycosyltransferases WbgL²⁰ and BgtA²¹ (Figure S1C).²²

The structure of MU-Type1A_{penta} was confirmed by NMR (Figure S2). Proton NMR resonances were assigned using H,H-COSY, H,H-NOESY, and ¹H,¹³C-HSQC NMR spectra. Anomeric configuration was confirmed by coupling constants. Regiochemistry (linkage) was confirmed with help of the H,H-NOESY spectrum.

¹H NMR (D₂O, 298 K, 600 MHz), δ [ppm] = 7.527 (*d*, ³J_{H,H} = 8.9 Hz, 1 H, Cum H-5); 6.958 (*dd*, ³J_{H,H} = 8.9 Hz, ⁴J_{H,H} = 2.4 Hz, 1 H, Cum H-6); 6.899 (*d*, ⁴J_{H,H} = 2.4 Hz, 1 H, Cum H-8); 6.044 (*d*, ³J_{H,H} = 1.1 Hz, 1 H, Cum H-3); 5.126 (*d*, ³J_{H,H} = 4.2 Hz, 1 H, Fuc H-1); 5.046 (*d*, ³J_{H,H} = 3.8 Hz, 1 H, GalNAc H-1); 4.991–4.978 (*m* (appears as a multiplet due to virtual coupling with Gal H-2 and H-3, which are strongly coupled (ABX system)), 1 H, 1Gal H-1); 4.585 (*d*, ³J_{H,H} = 7.6 Hz, 1 H, 3Gal H-1); 4.558 (*d*, ³J_{H,H} = 8.4 Hz, 1 H, GlcNAc H-1); 4.232 (*q*, ³J_{H,H} = 6.7 Hz, 1 H, Fuc H-5); 4.175 (*dd*, ³J_{H,H} = 6.2 Hz, ³J_{H,H} = 5.9 Hz, 1 H, GalNAc H-5); 4.112–4.108 (*m*, 1 H, 1Gal H-4); 3.725–3.707 (*m*, 1 H, GalNAc H-2); 4.083 (*dd*, ³J_{H,H} = 2.9 Hz, ³J_{H,H} < 1 Hz, 1 H, 3Gal H-4); 3.901 (*dd*, ³J_{H,H} = 10.6 Hz, ³J_{H,H} = 8.1 Hz, 1 H, GlcNAc H-3); 3.841 (*dd*, ³J_{H,H} = 3.3 Hz, ³J_{H,H} < 1 Hz, 1 H, GalNAc H-

4); 3.823 (*dd*, ³J_{H,H} = 7.0 Hz, ³J_{H,H} = 3.3 Hz, 1 H, GalNAc H-3); 3.814–3.781 (*m*, 3 H, 3Gal H-3, 1Gal H-5, GalNAc H-6a); 3.743–3.717 (*m*, 2 H, 1Gal H-2, 1Gal H-3); 3.724 (*dd*, ³J_{H,H} = 10.6 Hz, ³J_{H,H} = 8.4 Hz, 1 H, GlcNAc H-2); 3.699–3.663 (*m*, 4 H, GlcNAc H-6b, 3Gal H-2, 3Gal H-6a, 1Gal H-6a,b); 3.650–3.594 (*m*, 5 H, Fuc H-2, Fuc H-4, 1Gal H-6b, GalNAc H-6a,b); 3.537–3.522 (*m*, 2 H, 3Gal H-5, 3Gal H-6b); 3.503 (*dd*, ³J_{H,H} = 10.5 Hz, ³J_{H,H} = 3.4 Hz, 1 H, Fuc H-3); 3.422 (*dd*, ³J_{H,H} = 10.0 Hz, ³J_{H,H} = 8.1 Hz, 1 H, GlcNAc H-4); 3.422 (*ddd*, ³J_{H,H} = 10.0 Hz, ³J_{H,H} = 4.4 Hz, ³J_{H,H} = 2.2 Hz, 1 H, GlcNAc H-5); 2.251 (*d*, ⁴J_{H,H} = 1.1 Hz, 3 H, Cum H-11); 1.959 (*s*, 3 H, NHAc); 1.903 (*s*, 3 H, NHAc); 1.130 (*d*, ³J_{H,H} = 6.7 Hz, 3 H, Fuc H-6).

Constructing the EABase Expression System. A DNA cassette encoding both the EABase enzyme and an *N*-acetylhexosaminidase for the coupled reaction was constructed for coexpression from an appropriate expression vector in *E. coli*. First, the gene encoding *N*-acetylhexosaminidase from *Streptomyces plicatus* (SpHex)²³ was amplified by PCR reaction using the primers TAT ACA TAT GAC CAC CGG CGC CGC CCC GGA C and TAT AAG CTT TCA GGT CCA GGG CAC CTG CGG CGA G, and pET3-SpHex as the template. The PCR product was then cloned into the vector pTKNd (under the control of a constitutive promoter) by restriction sites NdeI and HindIII. An XhoI site within the SpHex gene was then removed by site-directed mutagenesis using the primers CTC CCG CCA CCT GGA GGT GGT CCC C and GGG GAC CAC CTC CAG GTG CGG GGA G (mutation underlined). This afforded the plasmid pTKNd-SpHex. Downstream of the SpHex gene, we cloned the EABase from either *Clostridium perfringens* or *Streptococcus pneumoniae* SP3-BS71 (CpGH98 and Sp3GH98, respectively) along with an upstream ribosome-binding site. The gene encoding CpGH98 along with the upstream ribosome-binding site was PCR amplified from a pET21-based vector encoding the gene^{5b} using the primers AAG TCG ACA AAT AAT TTT GTT TAA CTT TAA GAA GGA GA and GCT AGT TAT TGC TCA GCG G (the standard T7-terminator primer). The PCR product was cut with Sall and XhoI and ligated to pTKNd-SpHex which had been cut with the same enzymes, resulting in the plasmid pTKNd-SpHex+CpGH98. A similar construct encoding Sp3GH98 in place of CpGH98 was generated by excising the CpGH98 gene from pTKNd-SpHex+CpGH98 using NheI and XhoI restriction sites and cloning the Sp3GH98 gene, which was PCR amplified from pET28-Sp3GH98⁶ using primers AAG TCG ACA AAT AAT TTT GTT TAA CTT TAA GAA GGA GA and ATA TCT CGA GAA AAT GAA GTT CGA ATT CAA GAT TTC C, via the same restriction sites, resulting in the plasmid pTKNd-SpHex+Sp3GH98. We observed that expression levels of CpGH98 and Sp3GH98 from pTKNd-SpHex+CpGH98 and pTKNd-SpHex+Sp3GH98, respectively, were low, prompting us to clone the SpHex+CpGH98 and SpHex+Sp3GH98 cassettes into a pET29 vector. The SpHex+CpGH98 was excised from pTKNd-SpHex+CpGH98 using NdeI and XhoI sites and cloned into pET29 cut with the same enzymes, generating the plasmid pET29-SpHex+CpGH98. The Sp3GH98 gene was cloned via NheI and XhoI sites in place of the CpGH98 gene, which had been excised from pET29-SpHex+CpGH98 using the same enzymes. We found that Sp3GH98 exhibited better activity toward the MU-Type1A_{penta} substrate than CpGH98 (data not shown); therefore, pET29-SpHex+Sp3GH98 was used as the template for library generation.

In the first generation library, site-saturation mutagenesis was performed individually at each of positions 530, 559, 560, 561, 562, 592, and 624 using the pET29-SpHex+Sp3GH98 as a template, and the resulting mutants were pooled. Mutants 2.0-X1 and 2.0-X2 were generated by site-directed mutagenesis using primers GGT ATT TTC AGT ACA GAG AGT TAT TGG ATT TGG GCA AAT and ATT TGC CCA AAT CCA ATA ACT CTC TGT ACT GAA AAT ACC to introduce the N559S mutation into the variants 1.1-I02 (N592 V) and 1.2-O22 (N592S), respectively. The second round library was generated using either 2.0-X1 or 2.0-X2 as template and performing site-saturation mutagenesis individually at each of positions 530, 560, 561, 562, and 624 and then pooling the mutants. Third generation libraries were prepared using mutants from the second generation as templates. First, site-saturation mutagenesis was performed at position

592 and then, on the pool of site-saturation mutants, further site-saturation mutagenesis was performed at position 630, yielding libraries of mutants randomized at both positions. Mutants from the third generation served as templates for the fourth round library wherein site-saturation mutagenesis was performed similarly at positions 663 and 677. The final library was generated by error-prone PCR upon mutant 4A.1-D15 using the GeneMorph II random mutagenesis kit (Agilent Technologies) following the manufacturer's protocols to produce a library with an average of three mutations per gene.

Screening Mutant Libraries. The Rosetta 2 (DE3) strain of *E. coli* was transformed with a plasmid library (derived from pET29-SpHex+Sp3GH98) encoding Sp3GH98 mutants and plated on LB agar containing kanamycin and chloramphenicol. Using a QPix2 colony-picking robot (Molecular Devices), individual colonies were picked and inoculated into wells of 384-well plates (Corning, 3680), containing 50 μ L of LB (including 50 μ g/mL kanamycin and 35 μ g/mL chloramphenicol) per well. The 384-well culture plates were grown overnight at 37 °C without shaking. These plates served as master plates and after the addition of 10% DMSO could be frozen at -80 °C until needed. Enzyme expression was carried out at 30 °C in a shaking incubator in 96-deep well plates (Axygen, P-DW-20-C) using LBE-5052 autoinduction media²⁴ (800 μ L per well) containing kanamycin and including two sterile glass beads (3 mm diameter) per well to aid in mixing and aeration. A 96-pin microtiter plate replicator was used to inoculate four 96-deep well plates per 384-well master plate. Expression cultures in 96-deep well plates were grown at 30 °C overnight. Cells were harvested the following day by centrifuging the deep-well plates (4000 rpm, 10 min, 4 °C) and discarding the supernatant. Cells were washed by resuspension in assay buffer (50 mM sodium phosphate, 100 mM NaCl, pH 7.4) followed by centrifugation again (4000 rpm, 10 min, 4 °C), after which the supernatant was discarded. Cells were then resuspended in 25 μ L of 4 \times assay buffer (200 mM sodium phosphate, 400 mM NaCl, pH 7.4) to which "cOMplete, EDTA-free, protease inhibitor cocktail" (Roche), and Benzonase (EMD Millipore), and lysozyme (Sigma-Aldrich) had been added according to the manufacturers' recommendations. To the cell suspension, 25 μ L of a one-in-five dilution of 10 \times Bugbuster (EMD Millipore) into 4 \times assay buffer was added. The cells were allowed to lyse by incubation at room temperature (20 °C) for 20 min with occasional vortexing. The samples were diluted 2-fold by addition of 50 μ L of water. From each sample, 10 μ L were aliquoted into wells of a black 384-well plate (Corning, 3573) and then 10 μ L of 200 μ M MU-Type1A_{penta} was added to each well of the 384-well plate and the reactions were monitored by a Synergy HT plate reader (BioTek) using fluorescence detection with excitation at 380 nm and measuring emission at 454 nm.

Enzyme Kinetics. Using a coupled assay, stopped assays were performed at 30 °C using 1 μ M variant Sp3GH98 enzyme and between 0 and 2.5 mM MU-Type1A_{penta} in assay buffer (50 mM sodium phosphate, 100 mM NaCl, pH 7.4) including 0.05 mg/mL of SpHex and 0.05 mg/mL of β -galactosidase from *E. coli* (Figure S3A). At various time points, 10 μ L aliquots were taken from the assay mixtures and each added to 200 μ L of stop buffer (1 M glycine, pH 10.4). Fluorescence was measured using black 96-well microtiter plates (Corning, 3915) and compared to standards of 4-methylumbelliferone. Kinetics were also performed for wild-type Sp3GH98 and the 5E.3-N06 mutant using the substrate MU-Type2A_{tetra}, which bears the Gal β -1,4-GlcNAc linkage preferred by the Sp3GH98 enzyme (Figure S3B). For these assays similar conditions were used but the concentration of Sp3GH98 variants was 1 nM, and MU-Type2A_{tetra} concentration was varied between 5 and 200 μ M. β -Galactosidase was omitted from the coupled assay in the kinetics tests with MU-Type2A_{tetra}.

Structural Studies on Mutant Enzymes. In order to generate catalytically inactive variants of the evolved mutants for the solution of structures in complex with the type 1A and type 2A oligosaccharides (Figure S4), site-directed mutagenesis of the variants was performed to replace the catalytic acid residue, Glu558, with an alanine. This was done using the primers CAT GGT ATT TTC AGT ACA GCG AGT

TAT TGG ATT TGG GCA and TGC CCA AAT CCA ATA ACT CGC TGT ACT GAA AAT ACC ATG. Recombinant Sp3GH98 mutants were produced in *E. coli* and purified by immobilized metal affinity chromatography and gel filtration chromatography using procedures identical to those described for unmutated Sp3GH98.⁶ Protein concentrated to 20 mg/mL using a stirred ultrafiltration device with a 10 000 Da molecular weight cutoff membrane was crystallized using the hanging drop vapor diffusion method at 18 °C. Crystals were grown in 15–20% (v/v) polyethylene glycol 3350, 0.18–0.22 M ammonium sulfate, and 0.1 M sodium acetate trihydrate, pH 4.8. Crystals were soaked in the crystallization solution supplemented with a molar excess of blood group antigen for 20 min to produce product and substrate complexes. Crystals were flash-cooled with liquid nitrogen in crystallization solution supplemented with 20–30% ethylene glycol. Diffraction data was collected at 100 K at the Canadian Light Source on beamline 08B1-1 or on a home source comprising a MM-002 X-ray source coupled to Osmic "Blue" optics, an R-Axis 4++ detector, and an Oxford Cryosystems 700 cryostream. Diffraction data were processed with MOSFLM and AIMLESS.²⁵

The structure of monomeric wild-type Sp3GH98 (PDB ID 2WMI) was used as a molecular replacement search model in the program PHASER.²⁶ Models were manually corrected by successive rounds of building using COOT²⁷ and refinement with REMAC.²⁸ Waters were added automatically using the FINDWATERS function in COOT and checked manually. Carbohydrate ligands were modeled into maximum likelihood/ σ_a -weighted $F_o - F_c$ maps produced by refinement of the completed protein model prior to modeling of the carbohydrates. In all data sets, refinement procedures were monitored by flagging 5% of all observation as "free".²⁹ Model validation was performed with MOLPROBITY.³⁰ All data processing and model statistics are shown in Tables S2, S3, and S4. Structures deposited into the PDB archive include the apo structure of mutant 2.5-L19 (PDB ID 4d6c); 2.0-X01, 2.0-X02, and 2.5-L19, each in complex with the A-tetrasaccharide (PDB IDs 4d6e, 4d6d, 4d6g); 2.0-X01+E558A, 2.0-X02+E558A, and 2.5-L19+E558A, each in complex with the type 1 A-tetrasaccharide (PDB IDs 4d6f, 4d6h, 4d6i); and 2.0-X01+E558A, 2.0-X02+E558A, and 2.5-L19+E558A, each in complex with the type 2 A-tetrasaccharide (PDB IDs 4d6j, 4d71, 4d72).

Determining T_m of Sp3GH98 Variants. Variants of Sp3GH98 were prepared at 5 μ M in 50 mM sodium phosphate, pH 7.4, 100 mM NaCl. To 45 μ L aliquots of Sp3GH98 variants, was added SYPRO orange protein gel stain to 1 \times working concentration. In a DNA Engine thermocycler (Bio-Rad) equipped with a Chromo4 real-time detector (Bio-Rad), the samples were heated at a gradient between 25 and 99 °C at increments of one degree per minute, with fluorescence readings taken every minute. The T_m was determined from the fluorescence curves (Figure S5).

Detection of Antigen Removal by Immunofluorescence. Immunofluorescence tests (Figure S6) were carried out using A431 cells that had been fixed on glass slides (GeneTex, GTX25525). Wells on which the cells were fixed were treated with 11 μ M Sp3GH98 variants in 50 mM potassium phosphate, pH 7.5, 100 mM NaCl, and 30% dextran (40 kDa average molecular weight) and incubated for 4 h at 37 °C. For no enzyme controls, wells were incubated with buffered dextran only. Wells were washed three times with 5 min incubations with 50 mM potassium phosphate, pH 7.5, 100 mM NaCl. Then, 12 μ L of primary antibody (unpurified supernatants) was added to the wells and incubated overnight at 4 °C. The wells were washed again three times as before, and then incubated with 12 μ L of 30 μ g/mL FITC-labeled antimouse IgG or antimouse IgM and incubated at room temperature for 1 h. Wells were washed again three times, and allowed to dry before imaging under a microscope (Zeiss, Axioscop 2)

Assay of Antigen Removal from B Blood Group Erythrocytes Treated with Wild-Type Sp3GH98 and Mutant 5E.3-N06. Whole blood from healthy consenting donors was collected into a citrate Vacutainer using a protocol approved by the clinical ethics committee of the University of British Columbia. The tube was spun at 1000g for 4 min, and red blood cells (RBCs) were separated and washed 3 times with PBS buffer (pH = 7.4). For assays in the presence of 40k dextran, washed RBCs (200 μ L, 10% Hematocrit) were placed

in an eppendorf tube, and the supernatant was partially removed and replaced with PBS containing 40k dextran to a final concentration of 300 mg/mL of dextran. RBCs were mixed carefully and placed on an orbital shaker for 30 s. Diluted enzyme solutions were then added to a final volume of 200 μ L. The tubes were vortexed very gently, and placed on an orbital shaker for 1 h at room temperature (22 °C). After the reaction, RBCs were washed 3 times with an excess of PBS buffer (pH 7.0) and used for analysis using either hemagglutination plates or Micro Typing System (MTS) cards as described below. In assays with hemagglutination plates, the length of time for agglutination to be observed was taken as a measure of the degree of antigen removal, with a time of 30 min without agglutination indicating removal of antigenicity beyond detectability. In assays using MTS cards, the mobility of blood cells within gel columns containing immobilized antibodies was taken as a measure of antigen removal, translating into scores between 0 and 4 (higher scores indicating higher antigenicity). Quantitation of antigen removal by these methods is summarized in Table S5, and shown in Supporting Information Figure S7.

For analysis using hemagglutination plates, enzymatically treated and washed RBCs (100 μ L, 5% Hematocrit) were placed on a hemagglutination plate (Canadian Blood Service, P/N-J028183). Ten microliters of murine monoclonal antibodies (Dominion Biologicals Limited, Nova Scotia, Canada) was added as a separate drop beside the RBCs (yellow drops in Supporting Information Figure S7A and S7B). RBCs were mixed with antibody by manually flipping the plate, and agglutination time was determined visually when small aggregates of blood were formed: images of the RBCs were taken at different time points (Supporting Information Figure S7A and S7B). The experiment was conducted for 30 min to minimize the impact of water evaporation on experimental results.

For analysis using MTS cards, RBCs (12 μ L, 5% Hematocrit), suspended in diluent (MTS, Florida, USA), were added carefully to the mini gel column, leaving a space between the blood and the contents of the mini gel. The MTS cards were centrifuged at 156g for 6 min using a Beckman Coulter Allegra X-22R centrifuge with a modified sample holder as recommended. The extent of antigen removal from the surface of the RBC was evaluated from the location of RBCs in the mini gel after spinning according to the manufacturer's instructions. RBCs with a high surface antigen concentration (e.g., positive control) agglutinated upon interaction with the monoclonal antibody present in the gel column and could not penetrate (score 4+ in Supporting Information Figure S7). RBCs with no surface antigens (negative control and RBCs from which surface antigens have been completely removed) did not agglutinate and migrated to the bottom of the mini gel (score 0 in Supporting Information Figure S7C–D). RBCs that underwent partial removal of surface antigens migrated to positions between these and were assigned scores between 0 and 4 according to the manufacturer's instructions.

■ ASSOCIATED CONTENT

● Supporting Information

Tables S1–S5 and Figures S1–S7. This material is available free of charge via the Internet at <http://pubs.acs.org>.

■ AUTHOR INFORMATION

Corresponding Author

*withers@chem.ubc.ca

Notes

The authors declare no competing financial interest.

■ ACKNOWLEDGMENTS

We thank Dr. Henrik Clausen and Dr. Ulla Mandel for providing antibodies and for helpful discussions. D.H.K. is a recipient of CIHR and MSFHR research trainee postdoctoral fellowships. This research was funded by the Canadian Blood Services (CBS), the Canadian Institutes of Health Research (CIHR), and Health Canada. The infrastructure facility is

supported by the Canada Foundation for Innovation (CFI), the British Columbia Knowledge Development Fund (BCKDF), the Canada Research Chairs program, and the Michael Smith Foundation for Health Research (MSFHR). The authors thank the LMB Macromolecule Hub at the UBC Centre for Blood Research for the use of their research facilities. R.C. is a recipient of a (CIHR/CBS) postdoctoral fellowship in Transfusion Science, and a MSFHR postdoctoral trainee in Biomedical Research. J.N.K. is a recipient of a MSFHR career investigator scholar award. S.G.W. is a Tier-I Canada Research Chair in Chemical Biology.

■ REFERENCES

- (1) (a) Daniels, G.; Reid, M. E. *Transfusion* **2010**, *50*, 281–289. (b) Sazama, K. *Curr. Hematol. Rep.* **2003**, *2*, 518–521. (c) Carson, J. L.; Grossman, B. J.; Kleinman, S.; Tinmouth, A. T.; Marques, M. B.; Fung, M. K.; Holcomb, J. B.; Illoh, O.; Kaplan, L. J.; Katz, L. M.; Rao, S. V.; Roback, J. D.; Shander, A.; Tobian, A. A. R.; Weinstein, R.; McLaughlin, L. G. S.; Djulbegovic, B. *Ann. Int. Med.* **2012**, *157* (1), 49–U95. (d) Reid, M. E.; Lomas-Francis, C.; Olsson, M. L. *The Blood Group Antigen FactsBook*, 3rd ed.; Elsevier: New York, 2012.
- (2) Clausen, H.; Hakomori, S. *Vox Sang.* **1989**, *56*, 1–20.
- (3) Yamamoto, F.; Clausen, H.; White, T.; Marken, J.; Hakomori, S. *Nature* **1990**, *345*, 229–233.
- (4) (a) Goldstein, J.; Siviglia, G.; Hurst, R.; Lenny, L.; Reich, L. *Science* **1982**, *215*, 168–170. (b) Liu, Q. P.; Sulzenbacher, G.; Yuan, H.; Bennett, E. P.; Pietz, G.; Saunders, K.; Spence, J.; Nudelman, E.; Levery, S. B.; White, T.; Neveu, J. M.; Lane, W. S.; Bourne, Y.; Olsson, M. L.; Henrissat, B.; Clausen, H. *Nat. Biotechnol.* **2007**, *25*, 454–464. (c) Liu, Q. P.; Yuan, H.; Bennett, E. P.; Levery, S. B.; Nudelman, E.; Spence, J.; Pietz, G.; Saunders, K.; White, T.; Olsson, M. L.; Henrissat, B.; Sulzenbacher, G.; Clausen, H. *J. Biol. Chem.* **2008**, *283*, 8545–8554.
- (5) (a) Anderson, K. M.; Ashida, H.; Maskos, K.; Dell, A.; Li, S.-C.; Li, Y.-T. *J. Biol. Chem.* **2005**, *280*, 7720–7728. (b) Shaikh, F. A.; Randriantsoa, M.; Withers, S. G. *Biochemistry* **2009**, *48*, 8396–8404.
- (6) Higgins, M. A.; Whitworth, G. E.; El Warry, N.; Randriantsoa, M.; Samain, E.; Burke, R. D.; Vocadlo, D. J.; Boraston, A. B. *J. Biol. Chem.* **2009**, *284* (38), 26161–26173.
- (7) (a) Clausen, H.; Levery, S. B.; McKibbin, J. M.; Hakomori, S. *Biochemistry* **1985**, *24*, 3578–3586. (b) Clausen, H.; Levery, S. B.; Nudelman, E.; Baldwin, M.; Hakomori, S. *Biochemistry* **1986**, *25*, 7075–7085.
- (8) Prakobphol, A.; Leffler, H.; Fisher, S. J. *Crit. Rev. Oral Biol. Med.* **1993**, *4*, 325–333.
- (9) Scharchter, H.; Michaels, M. A.; Tilley, C. A.; Crookson, M. C.; Crookson, J. H. *Proc. Natl. Acad. Sci. U.S.A.* **1973**, *70*, 220–224.
- (10) Reetz, M. T.; Carballeira, J. D. *Nat. Protoc.* **2007**, *2* (4), 891–903.
- (11) Reetz, M. T.; Bocola, M.; Carballeira, J. D.; Zha, D. X.; Vogel, A. *Angew. Chem., Int. Ed.* **2005**, *44* (27), 4192–4196.
- (12) Chapanian, R.; Kwan, D. H.; Constantinescu, I.; Shaikh, F. A.; Rossi, N. A. A.; Withers, S. G.; Kizhakkedathu, J. N. Enhancement of biological reactions on cell surfaces via macromolecular crowding. *Nat. Commun.* **2014**, *5*, Article number: 4683.
- (13) (a) Olsson, M. L.; Hill, C. A.; de la Vega, H.; Liu, Q. P. *Transfus. Clin. Biol.* **2004**, *11*, 33–39. (b) Olsson, M. L.; Clausen, H. *Br. J. Haematol.* **2008**, *140*, 3–12.
- (14) Subramanian, V.; Ramachandran, S.; Klein, C.; Wellen, J. R.; Shenoy, S.; Chapman, W. C.; Mohanakumar, T. *Int. J. Immunogenet.* **2012**, *39*, 282–290.
- (15) Becker, L. E.; Süsal, C.; Morath, C. *Curr. Opin. Organ Transplant.* **2013**, *18*, 445–454.
- (16) (a) Dorling, A. *Am. J. Transplant.* **2011**, *12*, 545–553. (b) Bach, F. H.; Ferran, C.; Hechenleitner, P.; Mark, W.; Koyamada, N.; Miyatake, T.; Winkler, H.; Badrichani, A.; Candinas, D.; Hancock, W. E. *Nat. Med.* **1997**, *3*, 196–204. (c) Narayanan, K.; Jendrisak, M. D.; Phelan, D. L.; Mohanakumar, T. *Transpl. Immunol.* **2006**, *15*, 187–

197. (d) Lynch, R. J.; Platt, J. L. *Curr. Opin. Organ Transplant.* **2008**, *13*, 165–170.

(17) Sackmann, E. *Biological Membranes Architecture and Function*. In *Handbook of Biological Physics*; Lipowsky, R., Sackmann, E., Eds.; Elsevier: 1995; Vol. 1.

(18) (a) Randriantsoa, M. *Synthèse microbiologique des antigènes glucidiques des groupes sanguins*; Université Joseph Fourier: Grenoble, France, 2008. (b) Priem, B.; Gilbert, M.; Wakarchuk, W. W.; Heyraud, A.; Samain, E. *Glycobiology* **2002**, *12*, 235–240.

(19) Kim, Y.-W.; Lee, S. S.; Warren, R. A. J.; Withers, S. G. *J. Biol. Chem.* **2004**, *279* (41), 42787–42793.

(20) Engels, L.; Elling, L. *Glycobiology* **2014**, *24* (2), 170–178.

(21) Yi, W.; Shen, J.; Zhou, G.; Li, J.; Wang, P. G. *J. Am. Chem. Soc.* **2008**, *130* (44), 14420–14421.

(22) Kwan, D. H.; Ernst, S.; Kötzler, M. P.; Withers, S. G. *Glycobiology* **2015**.

(23) Williams, S. J.; Mark, B. L.; Vocadlo, D. J.; James, M. N. G.; Withers, S. G. *J. Biol. Chem.* **2002**, *277* (42), 40055–40065.

(24) Studier, F. W. *Protein Expr. Purif.* **2005**, *41*, 207–234.

(25) (a) Powell, H. R. *Acta Crystallogr., D: Biol. Crystallogr.* **1999**, *55* (Pt10), 1690–5. (b) Evans, P. R. *Acta Crystallogr., D: Biol. Crystallogr.* **2011**, *67* (Pt 4), 282–92.

(26) McCoy, A. J.; Grosse-Kunstleve, R. W.; Storoni, L. C.; Read, R. J. *Acta Crystallogr., D: Biol. Crystallogr.* **2005**, *61* (Pt 4), 458–64.

(27) Emsley, P.; Cowtan, K. *Acta Crystallogr., D: Biol. Crystallogr.* **2004**, *60* (Pt 12 Pt 1), 2126–32.

(28) Murshudov, G. N.; Vagin, A. A.; Dodson, E. J. *Acta Crystallogr., D: Biol. Crystallogr.* **1997**, *53* (Pt 3), 240–55.

(29) Brunger, A. T. *Nature* **1992**, *355* (6359), 472–5.

(30) Chen, V. B.; Arendall, W. B., 3rd; Headd, J. J.; Keedy, D. A.; Immormino, R. M.; Kapral, G. J.; Murray, L. W.; Richardson, J. S.; Richardson, D. C. *Acta Crystallogr., D: Biol. Crystallogr.* **2010**, *66* (Pt1), 12–21.